

# Glass Transition Behavior of Polystyrene Blocks in the Cores of Collapsed Dry Micelles Tethered by Poly(Dimethylsiloxane) Coronae in a PS-*b*-PDMS Diblock Copolymer

Er-Qiang Chen,<sup>\*,†,‡</sup> Yan Xia,<sup>‡</sup> Matthew J. Graham,<sup>†</sup> Mark D. Foster,<sup>†</sup> Yongli Mi,<sup>§</sup> Wen-Li Wu,<sup>||</sup> and Stephen Z. D. Cheng<sup>\*,†,‡</sup>

Maurice Morton Institute and Department of Polymer Science, The University of Akron, Akron, Ohio 44325-3909, Department of Polymer Science and Engineering, College of Chemistry and Molecular Engineering, Peking University, Beijing 100871, China, Department of Chemical Engineering, Hong Kong University of Science and Technology, Clear Water Bay, Kowloon, Hong Kong, China, and Polymer Division, National Institute of Standards and Technology, Gaithersburg, Maryland 20899

Received October 14, 2002. Revised Manuscript Received March 24, 2003

The micellization of a polystyrene-*b*-poly(dimethylsiloxane) (PS-*b*-PDMS) diblock copolymer with the number-average molecular weights ( $M_n$ ) of 193 000 g/mol for PS block and 39 000 g/mol for PDMS block and the glass transition behavior of the PS blocks in the cores of collapsed dry micelles with PDMS tethered coronae were studied. A range of micelle morphologies was observed by varying the micellization conditions and varying the ratio of the methylene chloride (MC) solvent and the *n*-dodecane (D) selective nonsolvent. MC is a solvent for both of the blocks, but D is a selective solvent for only the PDMS block. After completely removing the solvents below the glass transition temperature ( $T_g$ ) of the initially solvated PS blocks in MC via extraction and vacuum-drying, the collapsed dry micelles, which were originally spheres and cylinders, became “tablets” or “ribbons”. The diameters of the “tablets” and widths of the “ribbons” were approximately 50 and 100 nm, respectively. The thicknesses of these textures ranged from 20 to 40 nm. The PS block cores of the dried micelles exhibited a  $T_g$  very close to that of the homo-PS bulk samples with the same  $M_n$ . However, for a broad temperature range below the  $T_g^{\text{PS}}$ , the collapsed dry micelles possessed heat capacity ( $C_p$ ) values higher than the addition scheme calculated  $C_p$  based on PS and PDMS in their solid and liquid bulk states; whereas the  $C_p$  values of the liquid state above the  $T_g^{\text{PS}}$  fit well with the calculated data. These observations support the idea of PS interface layers with mobility induced by the liquid PDMS coronae such that only the inner cores of the PS blocks were in the glassy state. In a temperature region between 0 and 50 °C, the lower limit of the interface thickness (i.e., assuming that the mobile PS layers possessed the same mobility as the PS liquid) was estimated to be approximately 2 nm for the collapsed dry micelles. The interface thickness slightly increased with increasing temperature.

## Introduction

With the increasing demands of material applications for polymers, an understanding of their chemistry and physics in the condensed state has become a major topic of polymer materials research. Many physical phenomena, such as glass transition, crystallization, melting, mesophase transitions, submolecular and molecular relaxation processes, and viscoelastic behavior are traditionally defined in the condensed states of bulk polymers. But, one may ask whether these concepts defined for bulk structures and properties are still valid when it comes to the surfaces or interfaces of polymers? If not, at what size or dimension do these concepts break

down and what surface or interface relaxations dominate?

For example, the glass transition has been recently studied in different confined spaces such as thin films, in porous matrixes, and at or near the material surface.<sup>1–7</sup> Traditionally, a glass transition in a bulk describes a cooperative segmental motion of macromolecules on certain length and time scales.<sup>8</sup> To under-

\* Authors to whom correspondence should be addressed. E-mail: eqchen@pku.edu.cn or scheng@uakron.edu

<sup>†</sup> The University of Akron.

<sup>‡</sup> Peking University.

<sup>§</sup> Hong Kong University of Science and Technology.

<sup>||</sup> National Institute of Standards and Technology.

(1) Orts, W. J.; van Zanten, J. H.; Wu, W. L.; Satija, S. K. *Phys. Rev. Lett.* **1993**, *71*, 867.

(2) Wallace, W. E.; van Zanten, J. H.; Wu, W. L. *Phys. Rev. E* **1995**, *52*, R3329.

(3) Dalnoki-Veress, K.; Forrest, J. A.; Murray, C.; Gigault, C.; Dutcher, J. R. *Phys. Rev. E* **2001**, *63*, 031801.

(4) Forrest, J. A.; Dalnoki-Veress, K. *Adv. Colloid Interface Sci.* **2001**, *94* (1–3), 167.

(5) McKenna, G. B. *J. Phys. IV* **2000**, *10* (P7), 53.

(6) Hammerschmidt, J. A.; Gladfelter, W. L.; Haugstad, G. *Macromolecules* **1999**, *32*, 3360.

(7) Travinskaya, T.; Shilov, V.; Kovernik, G.; Klepko, V.; Lipatov, Y. S. *Composite Interfaces* **1999**, *6*, 297.

stand the effect of size limitation of a phase that still exhibits a bulk glass transition behavior, one can generate better-controlled, confined environments using diblock copolymers with two strongly segregating components. The variety of phase morphologies in diblock copolymers can provide templates with different confined dimensions and shapes. If the major component in a diblock copolymer has a higher glass transition temperature ( $T_g$ ) and the minor component possesses a lower  $T_g$ , the minor component is in a *hard* confinement constructed by the major component. When the confinement is on a nanometer length scale, it affects the  $T_g$  of the minor component.<sup>9</sup> On the other hand, a phase inversion would create a different environment in which the small glassy phase is surrounded by a liquid matrix. This could lead to a study of the effect of the liquid matrix on the glass transition behaviors of a small glassy phase.

It is known that polystyrene-*b*-poly(dimethylsiloxane) (PS-*b*-PDMS) diblock copolymers strongly segregate.<sup>10–12</sup> The Flory–Huggins interaction parameter  $\chi$  between PS and PDMS was estimated to be four times higher than that between PS and polyisoprene.<sup>10,11</sup> The  $T_g$  of PDMS is  $-127$  °C and its melting temperature ( $T_m$ ) is  $-54$  °C.<sup>13</sup> Both are much lower than the  $T_g$  of bulk PS which is  $100$  °C.<sup>13</sup> The studies of bulk glass transition behaviors of PS-*b*-PDMS have shown that although the PDMS blocks stay in a liquid state at temperatures above their  $T_m$ , the interface between the PS and PDMS domains remained sharp with a negligible amount of intermixing. As a result, the dilution effect of the PDMS blocks on the glass transition temperature of the PS blocks ( $T_g^{\text{PS}}$ ) may not be significant.

Regarding the different glass transition behaviors, three regimes in bulk PS-*b*-PDMS were reported based on the number-average molecular weights ( $M_n$ ) of the PS blocks.<sup>10</sup> First, when the  $M_n$  of the PS blocks exceeded  $39\,000$  g/mol, the  $T_g^{\text{PS}}$  and the change of heat capacity at  $T_g^{\text{PS}}$  ( $\Delta C_p$ ) were identical to those of bulk homo-PS (H-PS) with an identical  $M_n$ . However, the width of the glass transition ( $\Delta T_g$ ) was significantly larger (about twice as broad as that of H-PS). Second, when the  $M_n$  of the PS blocks was lower than  $8200$  g/mol, the  $\Delta T_g$  broadened and the  $T_g^{\text{PS}}$  was lower than that of the corresponding H-PS bulk samples. The corresponding  $\Delta C_p$  values were also different from those of H-PS. Third, when the  $M_n$  of the PS blocks was between  $8200$  and  $39\,000$  g/mol, the glass transition of PS blocks behaved between those two regimes. Because the PS-*b*-PDMS samples studied had the PS blocks ranging from  $24$  to  $86$  (wt) %, the equilibrium bulk morphologies were subject to changes from sphere to cylinder to lamella with increasing PS composition. As a result, the PS block morphology changed from a discontinuous to a continuous phase.

To study the effect that liquid molecules tethered to a small glassy phase have on polymer glass transition behaviors, a case was investigated where only very thin liquid molecular layers covered small glassy cores. It is known that block copolymers in selective solvents are able to form micelles made up of a dense insoluble core of one block and an outer, less dense shell of another soluble block regardless of the block sizes.<sup>14,15</sup> Furthermore, the micelles of a given diblock copolymer may present different morphologies depending upon the conditions under which the micellization took place. Complete solvent removal at a temperature near the initial  $T_g$  of the solvated core blocks can produce collapsed dry micelles that essentially retain their original shapes. To obtain a thin liquid layer on the surface of the rigid core, an asymmetric diblock copolymer containing a short block with a lower bulk  $T_g$  than that of the long block was selected.

PS-*b*-PDMS diblock copolymers with narrow molecular weight (MW) distributions for both blocks were found to form micelles in mixed solvents of *n*-alkanes and other selective solvents that solvate PDMS and not PS.<sup>16–19</sup> The prepared micelles possessed a PS core and a PDMS shell. The size and shape of the micelles were characterized by light scattering (LS), small-angle X-ray scattering (SAXS), and transmission electron microscopy (TEM).<sup>16–18</sup> It was observed that the micelles were generally spherical. Anomalous micelles of very large size, hollow spherical shape, and hollow cylindrical shape were also reported using the LS method.<sup>19</sup>

In our study, an asymmetric PS-*b*-PDMS diblock copolymer was chosen. A mixed solvent of methylene chloride (MC), a common solvent for both PS and PDMS blocks, and *n*-dodecane (D), a selective solvent for PDMS blocks, was utilized for the micellization of PS-*b*-PDMS. Various micelle morphologies for the PS-*b*-PDMS samples were observed depending upon the solvent/selective solvent volume ratio (MC/D), solution concentration, temperature, and processing conditions. When these micelles were dried their morphologies become unstable and they tried to relax back toward the equilibrium morphology in their corresponding bulk phases. To prevent this relaxation, the drying temperature must be lower than the  $T_g$  of the initially solvated PS blocks. Moreover, the  $M_n$  of PS blocks must be high enough to kinetically slow molecular rearrangement. Because the interface volume between the PS and PDMS blocks is significant compared to the volume of the bulk PS material in these micelles, the PDMS block effect on the glass transition behavior of the PS blocks in collapsed dry micelles could be quantitatively studied. The lower limit of the PS interface thickness was also estimated based on the heat capacity ( $C_p$ ) measurements below the  $T_g^{\text{PS}}$ .

(13) *Advanced Thermal Analysis System (ATHAS) Data Bank*. Pyda, M., Ed.; <http://web.utk.edu/~athas>.

(14) Webber, S. E.; Munk, P.; Tuzar, Z. *Solvents and Self-Organization of Polymers*; NATO ASI Series, Series E, Applied Sciences; Kluwer: Boston, MA, 1996; p 19.

(15) Hamley, I. W. *The Physics of Block Copolymers*, Oxford University Press: Oxford, U.K., 1998.

(16) Dawkins, J. V.; Taylor, G. *Makromol. Chem.* **1979**, *180*, 1737.

(17) Broadbent, G.; Brown, D. S.; Dawkins, J. V. *Polym. Commun.* **1987**, *28*, 282.

(18) Brown, D. S.; Dawkins, J. V.; Farnell, A. S.; Taylor, G. *Eur. Polym. J.* **1987**, *23*, 463.

(19) Iyama, K.; Nose, T. *Polymer* **1998**, *39*, 651.

(8) Debenedetti, P. G. *Metastable Liquids: Concepts and Principles*, Princeton University Press: Princeton, NJ, 1996.

(9) Zhu, L.; Chen, Y.; Zhang, A.; Calhoun, B. H.; Chun, M.; Quirk, R. P.; Cheng, S. Z. D.; Hsiao, B. S.; Yeh, F.; Hashimoto, T. *Phys. Rev. B.* **1999**, *60*, 10022.

(10) Krause, S.; Iskandar, M.; Iqbal, M. *Macromolecules* **1982**, *15*, 105.

(11) Chu, J. H.; Rangarajan, P.; Adams, L.; Register, R. A. *Polymer* **1995**, *36*, 1569.

(12) Rosati, D.; Perrin, M.; Navard, P.; Harbagiu, V.; Pinteala, M.; Simionescu, B. C. *Macromolecules* **1998**, *31*, 4301.

## Experimental Section

**Materials and Preparation of Micelles.** An asymmetrical PS-*b*-PDMS diblock copolymer was purchased from Polymer Source, Inc. (Dorval, PQ). The  $M_n$  of the PS and PDMS blocks were 193 000 g/mol and 39 000 g/mol, respectively. The MW distribution ( $M_w/M_n$ ) was 1.08. The molecular characterization data was provided by the material supplier and confirmed in our laboratory.

The copolymer was first dissolved in the common solvent MC ( $\text{CH}_2\text{Cl}_2$ ), with concentrations ranging between 1 and  $10 \times 10^{-2}$  g/mL. A selective solvent D, which dissolved only the PDMS blocks, was added to the solution to generate micelles. The composition of the common/selective solvent (MC/D) was controlled within a volume ratio from 1:1 to 1:6. Mild stirring for time periods exceeding 5 h was usually required to obtain a relatively uniform size distribution of micelles. The solvents were then evaporated at ambient atmosphere, and the collapsed dry micelles were collected. Because MC has a low boiling temperature of 40 °C, the swollen PS core could enter the glassy state relatively easily. This allowed the micelles to retain the morphologies formed during micellization. To completely remove D, which has a high boiling temperature of 216 °C, it was extracted using ethanol (with a boiling temperature of 78 °C) under ultrasonic agitation and stirring. All of the samples then underwent an annealing process in a vacuum at room temperature for 5 days followed by annealing at 50 °C for 1 day. Sufficient amounts of the dried micelles were then collected for  $C_p$  and weight loss measurements.

**Equipment and Experiments.** A transmission electron microscope (JEOL, JEM-1200 EX II) with an accelerating voltage of 120 kV was used for morphological studies. In addition, an atomic force microscope (AFM, Digital Nanoprobe III) in tapping mode was employed to characterize the shape, size, and topology of the dried micelles. A 100- $\mu\text{m}$  scanner was selected for both height and phase images. The force of the cantilever was small enough to limit its damage to the sample yet large enough to accurately explore surface features. The scanning rate ranged between 1 and 3 Hz. For microscopic observations, the micelle solutions were first spread on a clear water surface and then dried at room temperature. The dried micelles floating on the water surface were then transferred to the top of carbon-coated TEM grids and cover glass sides, respectively, for TEM and AFM observations after further drying processes.

The glass transition of the PS blocks was measured using a differential scanning calorimeter (Perkin-Elmer DSC-7).  $C_p$  measurements were taken in both the first and second heating scans. While the dried micelle samples were used in the first heating, the "fused" samples used in the second heating were initially heated to 160 °C, then isothermally annealed for 20 min, and finally cooled to -10 °C at 10 °C/min. The DSC temperature and  $C_p$  were calibrated, using standard indium and benzoic acid materials for the temperature calibration and standard sapphire single crystals for the  $C_p$  calibration, at different heating rates. The samples were sealed in aluminum pans with the pan weight identically matching the reference pan. Each measurement of  $C_p$  included three runs: the empty pans for baseline determination, the sapphire for  $C_p$  calibration, and the sample run.<sup>20</sup> The  $C_p$  was determined after the steady state was reached at a heating rate of 10 °C/min. Thermogravimetric analysis (TGA, TA2000 system) was used to confirm that the dried micelle samples were solvent free.

## Results and Discussion

**Morphologies of the PS/PDMS Micelles.** The PS-*b*-PDMS diblock copolymer used in this study was highly asymmetric with a PS block weight fraction of 83.1%. Considering the specific volumes of high-molecular weight PS and PDMS at 100 °C are 0.973<sup>21</sup> and

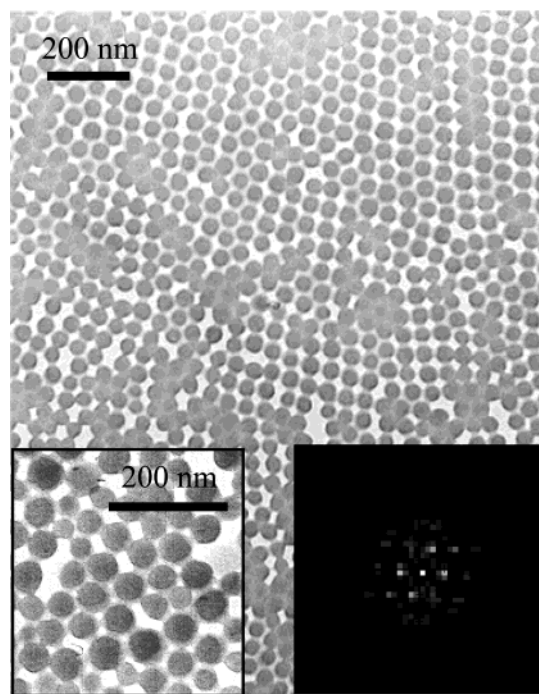


**Figure 1.** Bright-field TEM morphological images of the collapsed dry spherical micelles of the PS-*b*-PDMS at low magnifications. The lower left insert is the collapsed micelles under enlarged magnification in TEM and some of them are deformed to polygonal shapes. The lower right insert is the optical diffraction of this figure using the fast Fourier transformation method.

1.096 cm<sup>3</sup>/g,<sup>22</sup> respectively, the calculated volume fraction of the PS blocks in the copolymer is 81.6%. This means that the bulk equilibrium phase morphology of this diblock copolymer should be discontinuous spheres of PDMS blocks in a face-centered cubic packing within a continuous matrix of PS blocks.<sup>10</sup>

Figure 1 shows TEM micrographs of collapsed dry micelles ("tablets") that were prepared at room temperature with a PS-*b*-PDMS diblock concentration of  $2.5 \times 10^{-2}$  g/mL in a MC/D mixed solvent with a volume ratio of 1:2. These tablets are fairly uniform in size with a diameter of approximately 50 nm. The size is independent of the diblock copolymer concentrations studied in this mixed solvent. The lower left insert of Figure 1 presents a TEM image of the collapsed dry micelles at a higher magnification. The micelles stick to each other because of the liquid PDMS layers on their surfaces. The insert also shows that the tablets pack into a two-dimensional hexagonal lattice. The hexagonal lattice is evident in the optical diffraction pattern in reciprocal space, as seen in the lower right insert of Figure 1, obtained using a fast Fourier transformation. On the basis of different intensities of each diffraction spot, it can be deduced that the hexagonal lattice contains packing defects.

The diblock copolymer in a MC/D mixed solvent at a ratio of 1:6 produces different morphologies. The preparation of the solution included an initial dissolution of this copolymer in the MC/D mixed solvent at a ratio of 1:1 (with a concentration of  $8.75 \times 10^{-2}$  g/mL) and further addition of D solvent until the MC/D ratio

(20) Wunderlich, B. *Therm. Anal.*, Academic Press: Boston, MA, 1990.

(21) Richardson, M. J.; Savill, N. G. *Polymer* **1977**, *18*, 3.

(22) *Silicon Compounds: Register and Review*, 5th ed.; Huls America, Inc.: Piscataway, NJ, 1991; p 254.

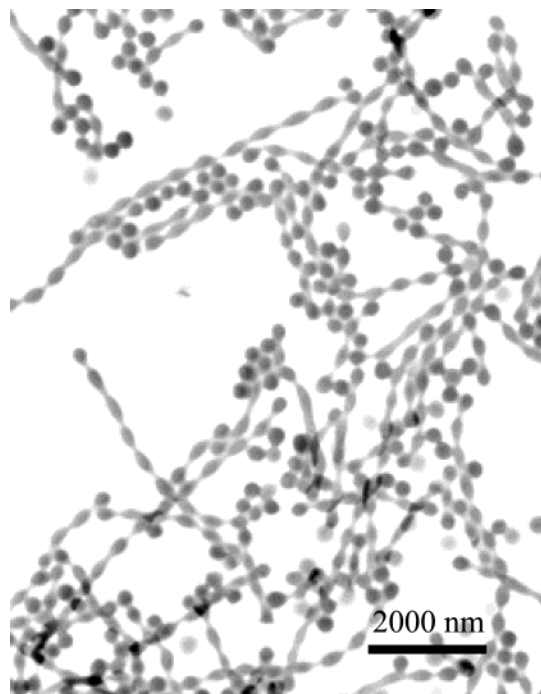


**Figure 2.** Bright-field TEM morphological images of the dried micelles of the PS-*b*-PDMS after micellization in the mixed solvent MC/D (1:6) at room temperature after being stirred for 6 h. The micelles exhibit a threading bead (“pearl-necklace-like”) morphology.

reached 1:6 (with a concentration of  $2.5 \times 10^{-2}$  g/mL). After the ethanol-extraction and 6 h of ultrasonic agitation with mild stirring at room temperature, a “pearl-necklace”-like morphology where the “pearls” are deformed was found as shown in Figure 2. The micelle diameter is twice as large ( $\sim 100$  nm) as those formed in the 1:2 ratio of the MC/D mixture (Figure 1). This morphology may serve as a transient metastable state between the formation of spheres and cylinders.<sup>23,24</sup>

By decreasing the micellization temperature to 0 °C, cylindrical micelles form in the same mixed solvent (MC/D 1:6). After D was extracted by ethanol using ultrasonic agitation and stirring, the cylinder micelles collapsed into “ribbons” as shown in Figure 3a. The micelle width is  $\sim 100$  nm and the length is a few micrometers. The stirring process during D extraction induces a necking phenomenon that results in observed ribbon entanglements and branches having widths of approximately 30 nm as shown in Figure 3b (see arrows). The widths of the necked ribbons are only  $1/3$ – $1/4$  of the original diameters which correlates to an elongation ratio of 9 to 16 if a constant volume is assumed. At a  $M_n$  of 39 000 g/mol and a degree of polymerization of 530, the fully extended PDMS block has a molecular length of only  $\sim 75$  nm. This implies that the PS blocks have to be responsible for this elongation process, as only the PS blocks can provide entanglements to sustain this deformation. In some cases, the deformation process leads to the breaking of cylinders in solution (see an arrow in the insert of Figure 3b). Necking is rare in samples that have undergone ethanol extraction and ultrasonic agitation without

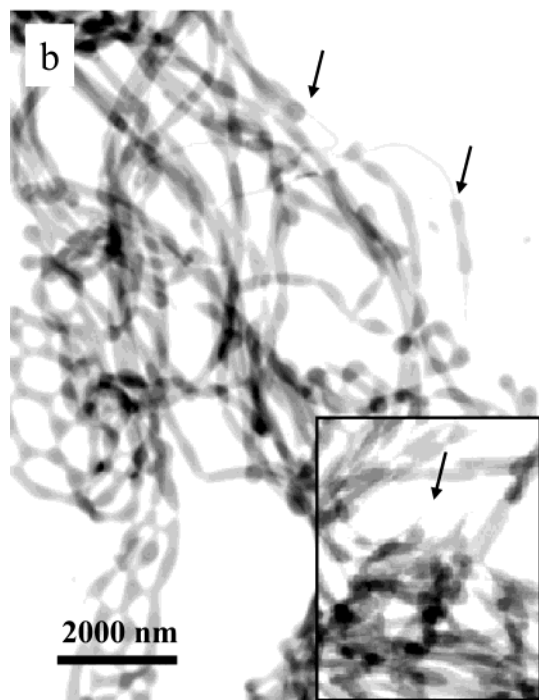
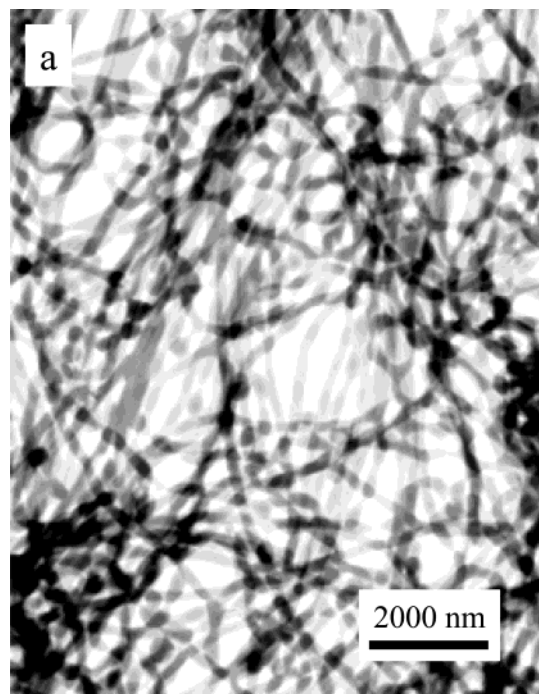


**Figure 3.** Bright-field TEM morphological images of the collapsed dry micelles of the PS-*b*-PDMS in the mixed solvent MC/D (1:6) at 0 °C: (a) collapsed cylinders, (b) necking of the cylinders (pointed by the arrows) after washing in ethanol using sonication. The insert in (b) shows the broken deformed cylinders (pointed by the arrow).

stirring. Combining this result with the morphology observed in Figure 2, it is speculated that the room-temperature stirring process must be near the initial solvated  $T_g^{PS}$  to cause the local periodic deformations. A detailed study of the morphological phase diagram for this diblock copolymer is currently being carried out and will be reported separately.<sup>25</sup>

(23) Cheng, S. Z. D.; Keller, A. *Ann. Mater. Sci.* **1998**, *28*, 533.

(24) Keller, A.; Cheng, S. Z. D. *Polymer* **1998**, *39*, 4461.

(25) Xia, Y.; Chen, E. Q.; Zhou, Z. K.; Mi, Y. L.; Wu, W. L. To be submitted for publication.

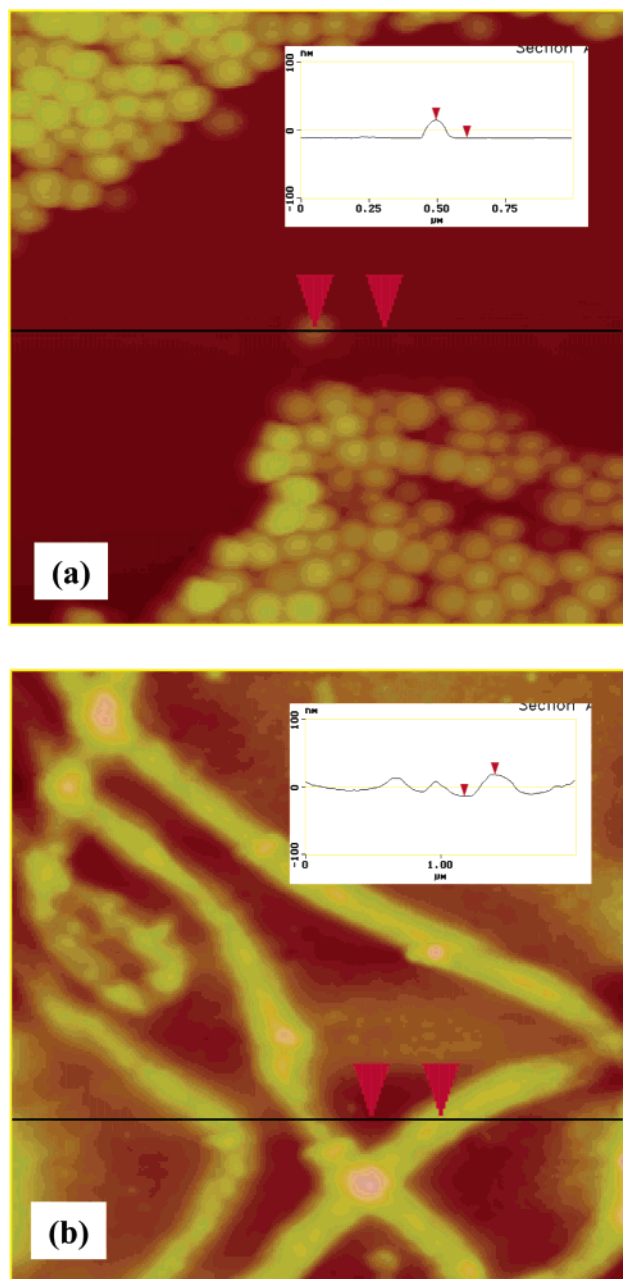


**Figure 4.** AFM micrographs of the collapsed dry spherical (a) and cylindrical (b) micelles. The cylinder after necking can be seen in (b). The inserts are the section analysis results, the vertical distances between two arrows are 26 and 31 nm for (a) and (b), respectively.

Previously, one PS-*b*-PDMS diblock copolymer was reported to generate micelles with hollowed vesicles in selective solvents. The LS measurements showed that the core diameters were much larger than the unperturbed end-to-end distance of the PS block.<sup>17</sup> However, Figures 2 and 3 show a uniform electron density within the ribbons suggesting these micelles are not hollow.

Figure 4 shows AFM images and surface topologies of collapsed dry spherical (tablets) and cylindrical (ribbons) micelles. After measuring different areas of the samples, the thicknesses of both the tablets and ribbons were found to be 20–40 nm. Their top free surfaces are rather flat. Considering a characteristic PS segment length of 0.757 nm,<sup>26</sup> the calculated unperturbed end-to-end distance of the PS blocks is ~33 nm.

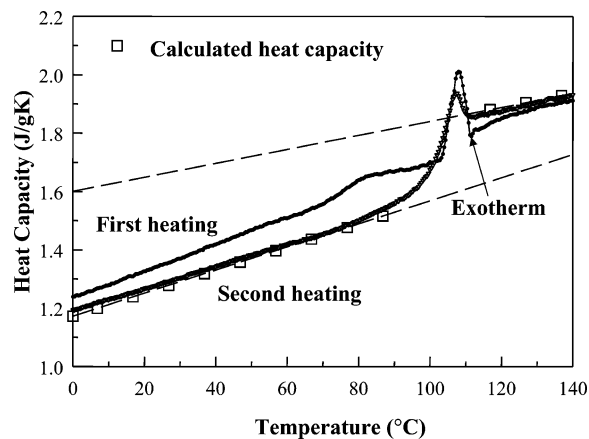


**Figure 5.**  $C_p$  data measured in the first and second DSC heating diagrams of the collapsed dry spherical micelles of the PS-*b*-PDMS.

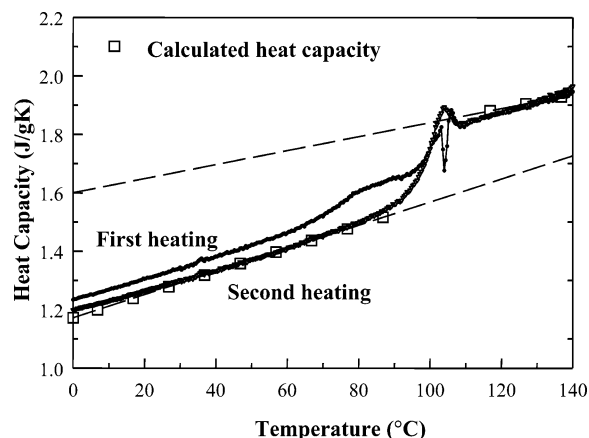


**Figure 6.**  $C_p$  data measured in the first and second DSC heating diagrams of the collapsed dry cylindrical micelles of the PS-*b*-PDMS.

On the basis of the sizes of the collapsed dry micelles, the PS blocks may not be severely stretched by the micellization and drying processes.

**Glass Transition of the PS Blocks in Dried PS-*b*-PDMS Micelles.** The  $C_p$  values in the  $T_g^{PS}$  region of these dried micelles were quantitatively measured. Complete removal of the solvent is indicated by the observation that less than 1% weight loss occurred in the sample at temperatures exceeding 220 °C for a heating rate of 5 °C/min during TGA. Further indications of complete solvent removal include that the  $T_g^{PS}$  of the collapsed dry micelles is very close to the  $T_g^{PS}$  of the homo-PS bulk samples with the same  $M_n$  (see below), and that the liquid state  $C_{pS}$  in these dried micelles are identical to the calculated values (see below).

Figures 5 and 6 present the  $C_p$  data measured in the first DSC heating of the tablets and ribbons at 10 °C/min. The second DSC heating diagrams in these two figures were measured after the micelle samples were heated to 160 °C for 20 min and then cooled to room temperature. Figure 5 shows the  $C_p$  data for the tablets, and Figure 6 is for the ribbons with only ethanol extraction and ultrasonic agitation. The  $C_p$  values of the bulk block copolymers were calculated via an addition

(26) Miyaki, Y.; Einaga, Y.; Fujita, H. *Macromolecules* **1978**, *11*, 1180.

scheme according to the weight fractions of the PS and PDMS blocks and  $C_p$  data recommended by ATHAS.<sup>13</sup> In this addition scheme, below the  $T_g^{PS}$ , the  $C_p$  data of the PS in the solid and the PDMS in the liquid are used to construct the overall  $C_p$  of the copolymer, whereas the overall  $C_p$  above the  $T_g^{PS}$  is calculated using  $C_p$  data of both the PS and PDMS in the liquid state. The results of the scheme are included in Figures 5 and 6 (square symbols).

The  $C_p$  data obtained in the second heating will be examined first. After first heating above the  $T_g^{PS}$ , the collapsed dry micelles fuse to each other and the system starts to relax toward its equilibrium bulk phase, i.e., the PS blocks become a continuous phase and the PDMS blocks form discontinuous spheres. After the samples were annealed at 160 °C for different periods of time ranging from a few minutes to a few hours, DSC results show that the measured  $T_g^{PS}$  is identical to that of H-PS of the same  $M_n$ . The  $C_p$  data of the second heating at temperatures both below and above the  $T_g^{PS}$  fit well to the calculated  $C_p$  based on the addition scheme. This indicates that the DSC experiments are insensitive to the detailed morphological grain sizes and orientation of the diblock copolymer as long as the PS blocks form the continuous phase. Furthermore, during the second heating, the fused PS-*b*-PDMS diblock copolymer exhibits a  $C_p$  difference ( $\Delta C_p$ ) at the  $T_g^{PS}$  of 0.24 J/(g·K). Because the  $\Delta C_p$  of pure PS is 0.29 J/(g·K),<sup>13,27–30</sup> the value of 0.24 J/(g·K) corresponds to the 83 (wt) % of PS in the PS-*b*-PDMS, which quantitatively agrees with the data obtained by the molecular analysis.

The  $C_p$  data of the first DSC heating diagrams of the collapsed dried micelles present features different from those of the second heating and the addition scheme calculation. In both the tablet (Figure 5) and ribbon (Figure 6) cases, the  $C_p$  value is higher than the value in the second heating and in the calculated  $C_p$  data between below 0 °C (the lower measured limit) and the  $T_g^{PS}$ . These higher  $C_p$  values remain until entering the  $T_g^{PS}$  region and overlap with an exothermic process evidenced by a slight decrease of the  $C_p$  value at 100 °C. In addition, broad endotherms appear at ~80 °C in both figures, which are attributed to thermal aging or enthalpy relaxation caused by the annealing at 50 °C during the drying process. Moreover, the first DSC heating diagrams in both figures exhibit apparently strong and sharp exotherms within or near the end of their  $T_g^{PS}$  regions. Above the  $T_g^{PS}$ , the  $C_p$  value reaches the liquid-state value. It has also been noticed that the  $T_g^{PS}$  values observed for these samples in the first heating are very close to that of the homo-PS bulk samples with the same  $M_n$ .

The  $T_g^{PS}$  values of H-PS latex with particle diameters ranging from 85 to 222 nm were studied in 1980.<sup>30</sup> Those H-PS particles presented complex thermal behaviors, similar to the first DSC heating diagrams shown in Figures 5 and 6. Because of the large surface areas of the particles, the exotherms at the  $T_g^{PS}$  were attributed to the particles fusing and releasing surface

tension.<sup>30</sup> In the present work, the sizes of the collapsed dry micelles are even smaller than the samples in the previous work, and they generate a larger amount of interface area before the fusion of these micelles. Note that the stress relaxation has an exothermic process with an energy of 2–4 J/g.<sup>31</sup> Therefore, the stress and interface tension release may explain the difference between the DSC first- and second-heating diagrams in Figures 5 and 6. This relaxation however, cannot cause the higher  $C_p$  data below the  $T_g^{PS}$ .

**Interfaces Between PS and PDMS Blocks.** In Figures 5 and 6, the  $C_p$  values of the first-heating diagrams in the temperature region below  $T_g^{PS}$  are 4–8% higher for the collapsed dry micelles compared to those obtained during the second heating and calculated data. The differences have been experimentally reproducible with five independent  $C_p$  measurements of the first heating runs for each sample at different heating rates ranging between 2.5 and 20 °C/min. Therefore, these  $C_p$  differences should be beyond the experimental error. A higher  $C_p$  supports the existence of local segmental motion in addition to the vibrational motion in the solid state. It is speculated that the strong thermal motion of the liquid PDMS blocks, each of which has one chain end tethered to the PS, affects the PS segmental motion at and near the interfaces despite the sharp interfaces between the PS and the PDMS blocks. As a result, extra PS segmental mobility on or near the interfaces may be introduced by the tethered PDMS blocks below the  $T_g^{PS}$ .

To estimate the amount of the mobile PS segments in the blocks at and near the interfaces, it is assumed that the PS-*b*-PDMS block copolymer phases possess an infinitely sharp interface boundary, and the inner core of PS blocks underneath the mobile PS segments are completely glassy. Moreover, when the mobile PDMS blocks affect the PS segment mobility at the interfaces, those PS segments possess the same mobility as they would in the amorphous liquid. Considering the mobility of the PS segments at the interfaces should most likely have a gradient toward its solid core centers, this estimation provides only a lower limit of the interface thickness.

The addition scheme was used to calculate  $C_p$ s in the case of solid PS and liquid PDMS blocks (0.35 J/(g·K)) and in the case of liquid PS and PDMS blocks (1.72 J/(g·K)) at 50 °C (to avoid thermal aging). The  $C_p$  difference between these two cases is 1.72 – 1.37 = 0.35 J/(g·K). However, the measured  $C_p$  of the tablets is 1.47 J/(g·K) at 50 °C, which is 0.1 J/(g·K) more than the calculated  $C_p$  [1.37 J/(g·K)]. Therefore, the population of the mobile PS blocks is estimated to be 29% (0.1 J/(g·K)/0.35 J/(g·K)) at this temperature. The same estimation made for the ribbons indicates that approximately 17% of the PS segments are mobile at 50 °C. This implies that the ribbons have a lower population of the mobile PS segments compared with that in the tablets as the latter possesses larger interface areas than the former.

Moreover, one may calculate the lower limit thickness of the mobile PS interface layer based on the population of the mobile PS segments and the geometrical dimension of the collapsed dry micelles. For the tablets at 50

(27) Karasz, F. E.; Bair, H. E.; O'Reilly, J. M. *J. Phys. Chem.* **1965**, *69*, 2657.

(28) Bair, H. E. *Polym. Eng. Sci.* **1970**, *10*, 247.

(29) Morese-Seguela, B.; St. Jacques, M.; Renaud, J. M.; Prud'homme, J. *Macromolecules* **1980**, *13*, 100.

(30) Gaur, U.; Wunderlich, B. *Macromolecules* **1980**, *13*, 1618.

(31) Cheng, S. Z. D.; Wunderlich, B. *Macromolecules* **1987**, *20*, 1630.

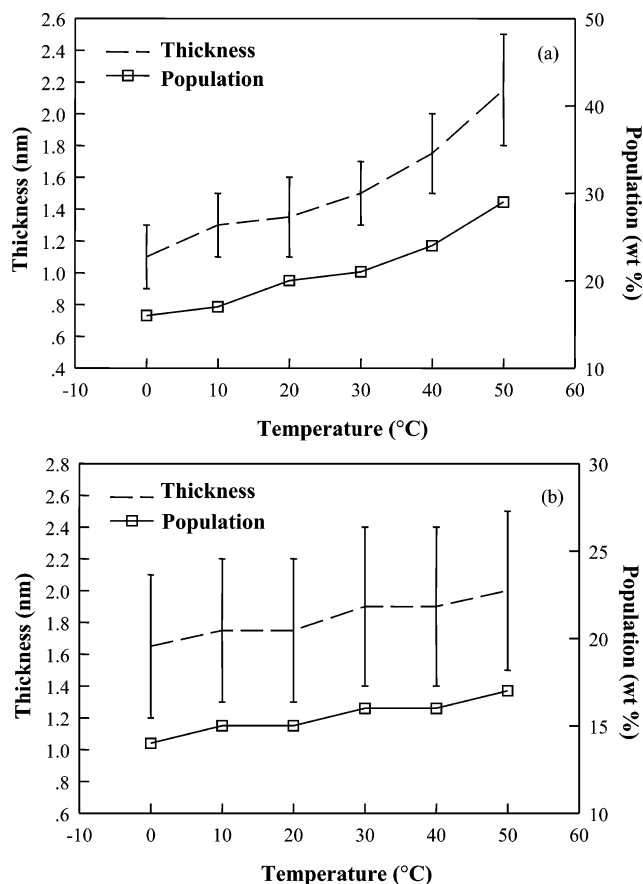


**Figure 7.** Populations of the mobile PS segments and lower limits of the interface thicknesses in the collapsed dry spherical (a) and cylindrical (b) micelles with respect to temperature. The surface area calculation is based on the diameter and thickness of the “tablet” and “ribbon”. Vertical bars represent the thicknesses corresponding to the calculated values using the heights of 20 and 40 nm, respectively.

°C with a diameter of 50 nm and a thickness of 20–40 nm, the lower limit thickness of the mobile PS layer is 1.8–2.5 nm. For the ribbons at 50 °C with a width of 100 nm and thicknesses of 20–40 nm, the lower limit thickness is 1.5–2.5 nm. Figure 7a and b illustrates the population of the lower limits of mobile PS layer thicknesses as functions of temperature for both types of collapsed dry micelles. The thickness of the mobile PS layer slightly increases with temperature. It is found that at the same temperature, both the tablets and ribbons present similar lower limit layer thicknesses. This indicates that the depth of the PS segmental motion induced by the tethered liquid PDMS blocks is insensitive to the shape of the collapsed dried micelles.

Considering that the PS segmental mobility may exhibit a gradient toward the PS solid cores, a diffused layer thickness between mobile and solid PS segments may exist. Nevertheless, the basic concept of an en-

hanced mobility layer at the interface remains true. The theoretical calculated interface thickness in block copolymers within the sharp, strongly segregated block regions is usually less than 2 nm. Semiquantitatively, the interfacial layer thickness can be predicated by  $a\chi^{-1/2}$ ,<sup>15</sup> where  $a$  is the statistical segment length, and  $\chi$  is the Flory interaction parameter. For this case the  $a$  for PS is 0.757 nm and the  $\chi$  is  $\sim 0.3$ ,<sup>11</sup> so the interface is estimated to be  $\sim 1.4$  nm. This interface thickness is slightly smaller than the lower limit deduced from the  $C_p$  data, indicating that the segmental mobility induced by the tethered liquid PDMS blocks may be slightly deeper than this interface.

## Conclusion

Various micelle morphologies can be observed by varying micellization conditions in an asymmetric PS-*b*-PDMS diblock copolymer with  $M_n = 193\,000$  g/mol for the PS blocks and  $M_n = 39\,000$  g/mol for the PDMS blocks. When MC and D are chosen as the common and selective solvents, the micelles generated have a liquid layer of PDMS blocks tethered to a core of PS blocks. Both the spherical and cylindrical morphologies of these micelles have been identified in solution. The cylindrical micelles also undergo necking during the stirring process. When the stirring temperature is close to the initial solvated  $T_g^{PS}$ , the “pearl-necklace”-like morphology can also be seen. Complete removal of the solvents at a temperature lower than the initial solvated  $T_g^{PS}$  produces collapsed dry micelles which retain their metastable morphologies. The collapsed spherical (“tablet”) and cylindrical (“ribbon”) micelles were approximately 50 and 100 nm in diameter and width, respectively; whereas their thicknesses were found to be 20–40 nm. Exothermic and endothermic processes in the DSC first-heating diagrams within the  $T_g^{PS}$  region are caused by the fusion of the micelles and the release of stress and interface tension. The quantitative  $C_p$  measurements of the collapsed dry micelles indicate that in a wide temperature region, the  $C_p$  values below  $T_g^{PS}$  are higher than those of the bulk (fused) samples. The increase in  $C_p$  is attributed to a detectable amount of the mobility imbued to the PS segments by the tethered liquid PDMS block in the collapsed dry micelles. Between 0 and 50 °C, the lower-limit layer thickness of the mobile PS segments is estimated to be approximately 1.5–2.5 nm for both the tablets and ribbons, which slightly increases with temperature.

**Acknowledgment.** This work was supported by NIST and the NSF (DMR-0203994). E.Q.C. acknowledges support from the National Natural Science Foundation of China (NSFC-20025414) which helped in the completion of this work.

CM021010X